IEEE Access
Multidisciplinary | Rapid Review | Open Access Journal

Received February 9, 2021, accepted February 24, 2021, date of publication February 26, 2021, date of current version March 8, 2021.

Digital Object Identifier 10.1109/ACCESS.2021.3062611

Exploring the Resilience of Uncertain Nonlinear Handling Chain Systems in Container Ports With a Novel Sliding Mode Control

BOWEI XU[1,2], JUNJUN LI[3], YONGSHENG YANG[1], HUAFENG WU[3], WEIHUI DAI[2], (Member, IEEE), AND OCTAVIAN POSTOLACHE[4], (Senior Member, IEEE)

[1]Institute of Logistics Science and Engineering, Shanghai Maritime University, Shanghai 201306, China
[2]School of Management, Fudan University, Shanghai 200433, China
[3]College of Merchant Marine, Shanghai Maritime University, Shanghai 201306, China
[4]Instituto de Telecomunicacoes, ISCTE-IUL, 1049-001 Lisbon, Portugal

Corresponding author: Junjun Li (jsliljj@163.com)

This work was supported by the National Social Science Foundation project of China under Grant 17CGL018.

ABSTRACT Uncertain handling chain system (HCS) of container ports brings steady-state error to the original control decisions, and even worse, dramatically degrades the system performance. The steady-state error will cause unsatisfied freight requirement to be much higher than the expected value for a long time, resulting in the decrease of system robustness and resilience. In this work, a novel sliding mode control with power integral reaching law (SMC-P) is presented for nonlinear HCS of container ports under uncertainty. Specifically, the integral of system state variable, the exponential reaching law and the power of the switching function are integrated to the traditional reaching law. And it is proven that the eliminated steady-state error, the accelerated approach speed, and the reduced chattering can be effectively obtained by SMC-P. A nonlinear HCS in container ports with uncertain freight requirement and handling ability is considered. SMC-P is compared with traditional method, genetic algorithm, quasi-sliding mode control and integral sliding mode control. Simulation results show that SMC-P does not only balance both steady-state error reduction and chattering avoidance caused by uncertainty, but also optimize the performance, robustness, and resilience of the uncertain nonlinear HCS. This study also brings economic and sustainability contributions for port authorities.

INDEX TERMS Resilience, uncertain nonlinear handling chain system, sliding mode control, power integral reaching law.

I. INTRODUCTION

Container ports are key elements of global port and shipping supply chains, providing connection between shipping-and-traffic -based transportation modes. Chinese ports play an important role in the maritime transport of containers, as stated in the results of the latest survey of Shanghai International Shipping Institute (updated to April 2020), in which there are seven Chinese ports ranked in the world top 10 container ports, in terms of number of handled containers. However, accompanied with the deterioration of the global economic and trade environment, container ports are facing more challenges, such as fiercer and fiercer competition, improving the service level, attracting freight source, saving operation cost, promoting operation efficiency (He etc., 2019) [1]. The resilient and efficient container handling chain system (HCS) has been presented as an opportunity to improve the operations and performances of container port simultaneously (Xu etc., 2019) [2]. Because of these benefits, the container handling chain system has attracted much attention from port authorities and other players in the port and shipping supply chain, and researchers worldwide.

The resilient and efficient HCS strongly relies on the following interactive coupling stages: the delivery/receipt of containers, the loading and unloading of yard cranes, the temporary storage of containers at the yard, the horizontal transportation of containers between berth and yard, the loading and unloading of gantry cranes, and the shipment of container vessel (Zheng *et al.*, 2019) [3]. These processes are very complex and dynamic. This concept has placed pressure on the management and maintenance of HCS today. In addition, HCS relates to the chaotic supply chain environment

The associate editor coordinating the review of this manuscript and approving it for publication was Baoping Cai.

(i.e., demand and cost fluctuation, severe weather, technical faults, trade policy), which imposes a high degree of uncertainty in making decisions about the system scheduling scheme. Furthermore, most previous works have neglected the fact that the port and shipping supply chains are increasingly affected by uncertainty, which leads to higher risk in the long term. Resilience has been widely discussed for various systems to reduce risks in dynamic environments (Feng etc., 2019) [4]. The system structure and maintenance resources are principal factors that affect its resilience (Cai *et al.*, 2018) [5]. For port authorities to be successful, it is becoming especially crucial to achieve higher resilience and efficiency in the management of container terminals within the context of HCSs.

A. LITERATURE REVIEW

In scientific literature, many contributions are available on the HCS of container ports, such as single-equipment scheduling, resources allocation and integrated scheduling (Han *et al.*, 2010; Luo *et al.*,2011; Said *et al.*,2015; Türkoğulları*et al.*, 2016) [6]–[9] in order to increase efficiency. Many methodologies, such as adopting new technologies, work organization models and information systems (Ballis *et al.*, 1997; Paixão *et al.*, 2003; Facchini *et al.*, 2017) [10]–[12] have been proposed to identify optimal solutions in the planning and management of container port HCS to reduce transit time and related operation costs. Traditionally, the HCS in container ports have been studied separately and independently for the three main machines. Because operations in container ports run synchronously, optimizing a particular aspect of the HCS cannot guarantee the improvement in the overall productivity of container port operations (Said *et al.*,2015) [8]. Integrated scheduling of container handling equipment is essential in improving the efficiency of container ports (Luo *et al.*,2011) [7]. Said *et al.* (2015) considered the container port as a global system instead of single optimization problems and optimized the container handling problems, quay crane assignment problem, yard crane assignment problem, and truck assignment problem simultaneously [8]. Liang *et al.* (2018) established a coupling model to solve the quay crane scheduling problem (QCSP) from two aspects: the task dispatch and quantity configuration of quay cranes [13]. However, most of these researches generally consider deterministic environment, whereas the uncertain factors are involved less.

In fact, container port operators must face to various uncertain factors and unknown issues. Hence, the uncertainty is naturally inevitable in the HCS of container ports. Uncertainty in HCS mainly includes vessel arrival time, task handling time, equipment reliability, infrastructure constraints, container information inaccuracy, handling resource unavailability, weather variability, etc (Iris *et al.*, 2019) [14]. These uncertainties will impact the initial schedule, cause extra cost, and degrade the actual operation performance of container port. More recently, much attention has been paid to container port uncertainty issue. One way to deal with these uncertainties include revision or rescheduling when uncertainty is realized, called the predictive-reactive approach (Aytug *et al.*, 2005) [15]. Considering the intra-/inter-port handling of the containers, Facchini *et al.* (2020) defined a mathematical model based on a computational algorithm for non-linear programming, in order to identify the number of containers to be stocked in port and/or in dry port, minimize the overall running costs and the carbon footprint and support decision makers in identifying the best strategy [16]. However, once the uncertainty occurs, the planners should adjust or reschedule the initial schedule to satisfy the reality. This adjustment or rescheduling incurs extra cost, and impacts the other plans or schedules. If the uncertainty can be considered in the initial schedule, the risk of adjusting schedules will be reduced significantly.

Other ways are to generate perturbation-insensitive robust schedules by considering uncertainties while making plans (Han *et al.*, 2010) [6]. Han *et al.* (2010) addressed berth and Quay Crane Scheduling Problem in a simultaneous way under uncertainties of vessel arrival time and container handling time [6]. Zhen (2013) considered yard template planning under uncertain vessel arrival times and berthing positions, and proposed a mixed integer programming model and a solution method [16]. Golias *et al.* (2014) presented a mathematical model and a solution approach for the discrete berth scheduling problem, where vessel arrival and handling times are not known with certainty [18]. Mhalla *et al.* (2016) presented a robust control strategy towards uncertainty for seaport handling equipments and tried to reduce unavailability of machines in transportation system and to minimize the total transfer time [19]. Zheng *et al.* (2019) investigated single yard crane scheduling to minimize the expected total tardiness of tasks, and focused on the case with uncertain release times of retrieval tasks [3]. Considering the uncertainty of vessel arrivals and the fluctuation in the container handling rate of quay cranes, Iris *et al.* (2019) developed a recoverable robust optimization approach for the weekly berth and quay crane planning problem and suggested a proactive baseline schedule with reactive recovery costs [14]. Considering uncertainty and traffic congestion, He *et al.* (2019) not only optimized the efficiency of YC operations, but also optimized the extra loss caused by uncertainty for reducing risk of adjusting schedule as the result of the task groups' arriving times and handling volumes deviating from their plan [1]. Up to present, most of literatures about uncertain HCS in container ports have been modeled from an operations research viewpoint. However, the vast majority disregard the operation resilience problem inherent in the uncertain HCS of container port.

B. MOTIVATIONS FOR WORK

A close container port handling chain is inevitable to reduce dwell times and improve service level and efficiency as far as possible. Since the entire container port system is capital intensive and complicated with lots of operation regulations, container port operators tend to establish an efficient HCS

and wish to maintain a resilient running of the whole system despite uncertainties.

The key feature of a HCS lies in that there are various uncertain factors and unknown issues in the whole container port operation, which brings the following main difficulties. Firstly, uncertainties make the HCS modeling more complicated, dynamic, and inevitable in the practice of container ports (Xu *et al.*, 2019) [2]. Secondly, system performance may be degraded by the affection of presence of nonlinearities and external disturbances (Han *et al.*, 2017) [21]. Thirdly, the actual HCS in container ports requires small steady-state error, fast and good robustness, strong resilience, which has led great difficulties to design an appropriate control strategy. The control approaches can improve the performance by optimizing control decisions on the system behaviors (Xu *et al.*, 2019; 2020) [2], [20]. In these cases, it can be observed how the system behaviors can vary and what are the effects of control decisions. As such, a great number of control techniques have been proposed for uncertain nonlinear systems, see e.g. (Incremona *et al.*, 2015; Khanzadeh *et al.*, 2017; Mobayen *et al.*, 2018; Wang *et al.*, 2020) [22]–[25]. A robust SMC for uncertain discrete singular systems with time-varying delays and external disturbances was investigated [21]. A design theory of the finite-time robust-tracking composite nonlinear feedback controller was proposed for the fast synchronization and performance improvement of the uncertain chaotic systems of master-slave Chua (Mobayen *et al.*, 2018) [24]. However, in our knowledge very few researches have been published yet (August 2020) on the robustness and resilience of the nonlinear HCS in case of uncertainty of container ports.

Sliding mode control (SMC) is widely adopted in lots of complex and engineering systems, including the underactuated system, dynamical networks, underwater vehicles, robotics and spacecrafts, the inverted pendulum system, (Mobayen *et al.*, 2014; Incremona *et al.*, 2015; Khanzadeh *et al.*, 2017; Wang *et al.*, 2018) [22], [23], [26], [27]. It has the superiorities, such as fast response, insensitiveness, robustness and good tracking properties against parametric perturbations or model uncertainties or unknown disturbances (Mobayen *et al.*, 2011; Han *et al.*, 2017; Zhang *et al.*, 2018) [21], [28], [29]. However, SMC approach suffers from an important drawback of chattering. Mobayen *et al.* (2017) investigated a novel nonsingular fast terminal sliding-mode control method for the stabilization of the uncertain time-varying and nonlinear third order systems. Moreover, knowledge about the upper bounds of the disturbances was not required and the chattering problem was eliminated [30]. Quasi-sliding mode control has been proven to be an effective and efficient robust control technique to deal with nonlinearities, uncertainties, and chattering effects (Liu *et al.*, 2017) [31], but brings great steady-state error, which is not feasible in practice.

In summary, few scholars have considered the uncertainty in the nonlinear HCS of container ports from a control viewpoint (Xu *et al.*, 2019; 2020) [2], [20], which is the core of this work. It is very constructive and meaningful to use control techniques to evaluate the robustness and resilience of the HCS in case of uncertainty of container ports, since in many real cases the freight demand of containers might vary due to many different aspects. Therefore, this research has been done to fill these gaps and support container port operators in identifying the optimal control decisions.

C. CONTRIBUTIONS

Motivated by the aforementioned concerns, we further developed a sliding mode control with power integral reaching law (SMC-P) to deal with the HCS of container ports with nonlinearities and external disturbances, which not only gets rid of the chattering phenomena induced by the traditional sliding mode control but also eliminates the steady-state error of the system.

The major contributions of this work are multi-fold. To the best of our knowledge, a SMC-P is presented for the uncertain nonlinear HCS of container ports for the first time. There are some studies that focus on traditional operation optimization of the HCS. This study goes beyond these studies by evaluating the performance, robustness, and resilience of the uncertain nonlinear HCS of container ports with a control approach. Compared with the existing control approaches, the integral of system state variable, the exponential reaching law, and the power of the switching function are integrated to the traditional reaching law for accelerating the approach speed, reducing the chattering, and eliminating the steady-state error.

This study also brings practical contributions for port authorities. The extra losses, such as unsatisfied freight requirement, container arrive rate, steady-state error, and resilience, caused by uncertainty are measured. Simulation studies demonstrate the effectiveness of the proposed SMC-P by comparing with traditional method, genetic algorithm, quasi-sliding mode control and integral sliding mode control. Ports can analyze and manage the uncertain nonlinear HCS more resiliently and efficiently through the proposed method, and this would contribute to economic and sustainability efforts of container ports.

II. UNCERTAIN NONLINEAR HANDLING CHAIN SYSTEM IN CONTAINER PORTS

A. NONLINEAR MODEL

Nonlinear model of handling chain system in container ports is shown in FIGURE 1. For detailed description of the handling chain system in container ports, we refer the readers to Xu *et al.* (2019) [2]. Notation and variable are detailed in TABLE 1. In the following work, uppercase and lowercase words, such as *FR* and *fr*, are used in the frequency and time domains, respectively. There are two nonlinear segments in this model: the value of $arate(t)$ can't be less than 0, and there is an upper limit value $COMRATE_{\mathrm{m}}$ for $comrate(t)$ because of the actual limited handling ability. It is more complex and difficult to tune the control parameters during system operation in the nonlinear model for enhancing the service level and operation performance.

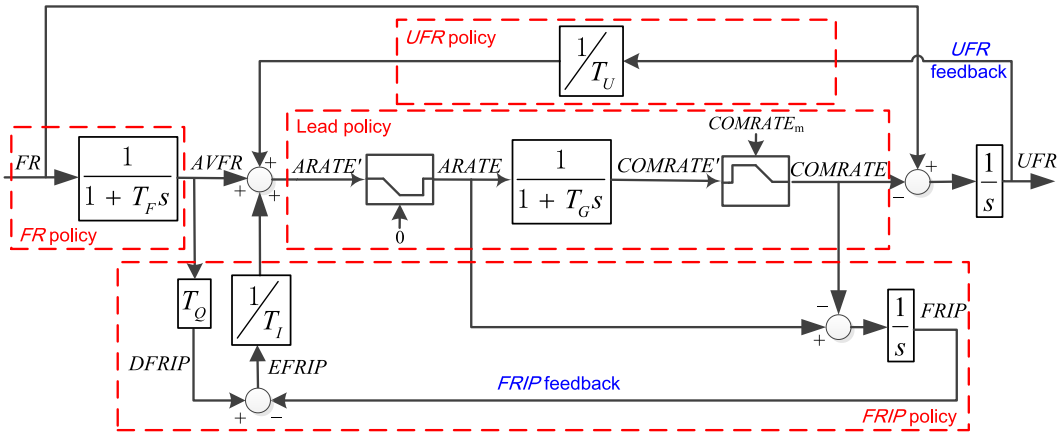

FIGURE 1. Nonlinear model of handling chain system in container ports.

TABLE 1. Notation and variable.

FR	Freight requirement	*AVFR*	Average *FR*	*UFR*	Unsatisfied *FR*
FRIP	*FR* in process	*EFRIP*	Error in *FRIP*	*DFRIP*	Desired *FRIP*
ARATE'	Arrive rate	*ARATE*	Nonnegative arrive rate	*COMRATE*'	Container handling completion rate
$COMRATE_{\mathrm{m}}$	An upper limit value of container handling completion rate	*COMRATE*	Container handling completion rate which satisfies the upper limit of handling capacity	T_U	Adjustment time of *UFR*
T_F	Time constant of FR forecast	T_G	Real lead-time of handling operations	T_Q	Expected lead-time of handling operations
T_I	Adjustment time of *EFRIP*	$\frac{1}{1+T_F s}$	Freight requirement policy	$\frac{1}{1+T_G s}$	Lead policy of handling operation
f_1	Uncertainty disturbances of the freight requirement	f_2	Uncertainty disturbances of the handling ability	*ITAE*	Integrated time and absolute error

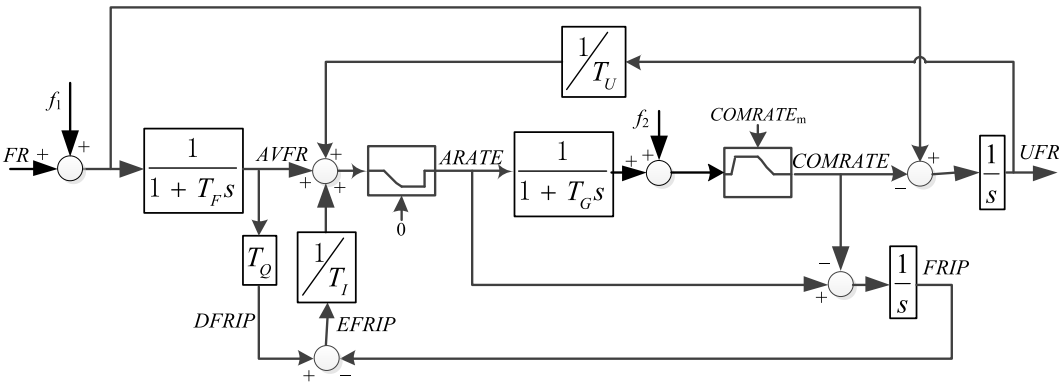

FIGURE 2. Uncertain nonlinear model of handling chain system in container ports.

B. UNCERTAIN NONLINEAR MODEL

Freight requirement and handling ability in container ports are usually uncertain. They prevail in real port operations. For more visualization, f_1 and f_2 represent the uncertainty disturbances of the freight requirement and the handling ability respectively in FIGURE 2.

From FIGURE 2, if $comrate(t)$ is less than or equal to $COMRATE_{\mathrm{m}}$, then

$$\frac{FR(s)+F_1(s)-\frac{ARATE(s)}{1+T_G s}-F_2(s)}{s}=UFR(s) \tag{1}$$

It is set that $F_{un}(s)=FR(s)+F_1(s)-F_2(s)$, $f_{un}(t)=fr(t)+f_1(t)-f_2(t)$, $u(t)=arate(t)$ (in this uncertain nonlinear HCS, $arate(t)$ is the control signal), $x_1(t)=ufr(t)$. To describe simply, "(t)" is omitted in the following text. Then, $f_{un}+T_G\cdot df_{un}/dt-arate=dx_1/dt+T_G\cdot d^2x_1/dt^2$. It is set that $x_2=dx_1/dt$, then the state equations are:

$$dx_1/dt=x_2 \tag{2}$$

$$dx_2/dt=(f_{un}+T_G\cdot df_{un}/dt-u-x_2)/T_G \tag{3}$$

III. QUASI-SLIDING MODE CONTROL AND STEADY-STATE ERROR

Sliding mode control (SMC) has been widely applied to many kinds of uncertain nonlinear control system. However, there's a drawback of chattering, which can be effectively

eliminated by quasi-sliding mode control [31]. In this section, we will establish quasi-sliding mode control and check its steady-state error.

A. QUASI-SLIDING MODE CONTROL

The linear switching function, (4), is employed:

$$s = c_1 x_1 + x_2 \tag{4}$$

The time derivative of s is:

$$\begin{aligned}\frac{ds}{dt} &= c_1 \frac{dx_1}{dt} + \frac{dx_2}{dt} \\ &= (c_1 - \frac{1}{T_G})x_2 + \frac{1}{T_G}(f_{un} + T_G \frac{df_{un}}{dt} - u)\end{aligned} \tag{5}$$

Here, $u-$ and $u+$ are used to denote the upper and lower limits of $u(t)$, respectively. Due to $T_G > 0$, (6) and (7) will definitely be established according to the generalized sliding mode condition.

$$(c_1 - \frac{1}{T_G})x_2 + \frac{1}{T_G}[f_{un} + T_G \frac{df_{un}}{dt} - u_+] < 0 \tag{6}$$

$$(c_1 - \frac{1}{T_G})x_2 + \frac{1}{T_G}(f_{un} + T_G \frac{df_{un}}{dt} - u_-) > 0 \tag{7}$$

To satisfy two nonlinear segments, it is set that $u_- = 0$ and $u_+ = COMRATE_{\mathrm{m}}$ [20]. To make the sliding mode area as large as possible, it is set that

$$c_1 = 1/T_G \tag{8}$$

Substituting (8) into (5), then it can be derived that

$$ds/dt = (f_{un} + T_G \cdot df_{un}/dt - u)/T_G \tag{9}$$

The reaching law can improve the dynamic quality of the reaching motion. To effectively reduce chattering, the exponential reaching law based on the saturation function is employed:

$$\frac{ds}{dt} = \begin{cases} -\varepsilon \cdot sign(s) - k \cdot s, & |s| > \Delta \\ -\varepsilon \cdot s/\Delta - k \cdot s, & |s| \le \Delta \end{cases} \tag{10}$$

where $\varepsilon > 0$, $k > 0$, Δ is a small positive real number. When the system stabilizes, s is generally located in its boundary layer. Then

$$\frac{ds}{dt} = -\frac{\varepsilon}{\Delta}s - k \cdot s = \frac{1}{T_G}(f_{un} + T_G \frac{df_{un}}{dt} - u) \tag{11}$$

Since the uncertain components f_1 and f_2 are unknown, they are not considered when calculating the output of the sliding mode controller. Then

$$u = fr + T_G(dfr/dt + \varepsilon \cdot s/\Delta + k \cdot s) \tag{12}$$

B. STEADY-STATE ERROR ANALYSIS

Substituting (12) into (9), then it can be derived that

$$\frac{ds}{dt} = \frac{1}{T_G}(f_{un} - fr) + \frac{d(f_{un} - fr)}{dt} - \frac{\varepsilon}{\Delta}s - ks \tag{13}$$

Let $\Delta f(t) = f_1(t) - f_2(t), f_h = \Delta f/T_G + d\Delta f/dt$, then

$$ds/dt = f_h - \varepsilon \cdot s/\Delta - ks \tag{14}$$

Take the Laplace transform on both sides of the above (14). To avoid confusion, use v instead of s as the complex variable in Laplace transform function.

$$v \cdot S(v) = F_h(v) - (\varepsilon/\Delta + k)S(v) \tag{15}$$

$$S(v) = F_h(v)/(v + \varepsilon/\Delta + k) \tag{16}$$

By means of application of the final value theorem, there are

$$\lim_{t\to\infty} f_h(t) = \lim_{v\to 0} v \cdot F_h(v) \tag{17}$$

$$\begin{aligned}\lim_{t\to\infty} s(t) &= \lim_{v\to 0} v \cdot S(v) = \lim_{v\to 0} v \cdot F_h(v)/(v + \varepsilon/\Delta + k) \\ &= \lim_{t\to\infty} f_h(t) \cdot \lim_{v\to 0} \frac{\Delta}{\Delta(v + k) + \varepsilon} \\ &= \frac{\Delta}{\varepsilon + \Delta \cdot k} \lim_{t\to\infty} f_h(t)\end{aligned} \tag{18}$$

If $f_{h1} \le \lim_{t\to\infty} f_h(t) \le f_{h2}$, then

$$\frac{\Delta}{\varepsilon + \Delta \cdot k} f_{h1} \le \lim_{t\to\infty} s(t) \le \frac{\Delta}{\varepsilon + \Delta \cdot k} f_{h2} \tag{19}$$

From (2), (4) can also be expressed as

$$s = c_1 x_1 + dx_1/dt \tag{20}$$

After performing Laplace transform on both sides of (20), it can be obtained that

$$S(v) = c_1 \cdot X_1(v) + v \cdot X_1(v) \tag{21}$$

And it can be deduced that

$$X_1(v) = S(v)/(c_1 + v) \tag{22}$$

Using the final value theorem, we get

$$\begin{aligned}\lim_{t\to\infty} ufr(t) &= \lim_{t\to\infty} x_1(t) = \lim_{v\to 0} \frac{v \cdot S(v)}{c_1 + v} \\ &= \lim_{v\to 0} v \cdot S(v) \cdot \lim_{v\to 0} \frac{1}{c_1 + v} \\ &= \frac{1}{c_1} \lim_{t\to\infty} s(t) = \frac{\Delta}{c_1(\varepsilon + \Delta \cdot k)} \lim_{t\to\infty} f_h(t)\end{aligned} \tag{23}$$

$$\frac{\Delta}{c_1(\varepsilon + \Delta \cdot k)} f_{h1} \le \lim_{t\to\infty} ufr(t) \le \frac{\Delta}{c_1(\varepsilon + \Delta \cdot k)} f_{h2} \tag{24}$$

If $\lim_{t\to\infty} f_h(t) \neq 0$, the steady-state error cannot be eliminated by using the saturation function.

IV. SLIDING MODE CONTROL WITH POWER INTEGRAL REACHING LAW

The commonly used method to reduce steady-state error is integral sliding mode control (ISMC) (Shideh etc., 2019) [32]. In ISMC, the switching function is $s = c_1 x_1 + x_2 + c_2 \int x_1 dt$. However, ISMC just increases the integral of the system state variable in the switching function, and no measures are taken for the reaching process. In this section, the reaching law is improved by adding the integral of the system state variable in the reaching law and enhancing the reaching strength to eliminate the steady-state error.

A. REACHING LAW BASED ON INTEGRAL OF x_1

If the reaching law employs the integral of x_1, that is $ds/dt = -k_i|\int_0^t x_1 d\tau|sgn(s)$. Where k_i is the integration coefficient, $k_i > 0$. To satisfy the generalized sliding mode condition ($s \cdot ds/dt < 0$), the absolute value sign is added to the integral of x_1, they multiply with the sign function $sgn\ (s)$, and the negative sign is added.

Similar to the calculation of u in (12), there is

$$u = fr + T_G\frac{dfr}{dt} + k_i T_G|\int_0^t x_1 d\tau|sign(s) \tag{25}$$

Substituting (25) into (9), we can get

$$\begin{aligned}\frac{ds}{dt} &= \frac{f_{un} - fr}{T_G} + \frac{df_{un}}{dt} - \frac{dfr}{dt} - k_i|\int_0^t x_1 d\tau|sign(s)\\ &= f_h - k_i|\int_0^t x_1 d\tau|sign(s)\end{aligned} \tag{26}$$

Take the Laplace transform on both sides of (26), then

$$v \cdot S(v) = F_h(v) - k_i|X_1(v)/v|sign(s) \tag{27}$$

It can be deduced that $X_1(v) = \pm\frac{vF_h(v) - v^2 \cdot S(v)}{k_i sign(s)}$. From (22) and (27), the steady-state error of *ufr* can be obtained by the following equations:

$$v \cdot S(v) = F_h(v) - k_i|\frac{S(v)}{v(c_1 + v)}|sign(s) \tag{28}$$

$$S(v) = \frac{\pm v(c_1 + v)F_h(v)}{k_i sign(s) \pm v^2(c_1 + v)} \tag{29}$$

$$\begin{aligned}\lim_{t\to\infty} s(t) &= \lim_{v\to 0} v \cdot S(v) = \lim_{v\to 0} \frac{\pm v^2(c_1 + v)F_h(v)}{k_i sign(s) \pm v^2(c_1 + v)}\\ &= \lim_{v\to 0} vF_h(v) \cdot \lim_{v\to 0} \frac{\pm v(c_1 + v)}{k_i sign(s) \pm v^2(c_1 + v)}\\ &= \lim_{t\to\infty} f_h(t) \cdot \lim_{v\to 0} \frac{\pm v(c_1 + v)}{k_i sign(s) \pm v^2(c_1 + v)} = 0\end{aligned} \tag{30}$$

$$\lim_{t\to\infty} ufr(t) = \lim_{t\to\infty} x_1(t) = \frac{1}{c_1}\lim_{t\to\infty} s(t) = 0 \tag{31}$$

In summary, the integral used in reaching law can effectively eliminate the steady-state error.

B. POWER INTEGRAL REACHING LAW

If there is only an integral in the reaching law, the reaching speed is slower in the beginning because the value of the integral gradually increases over time. To improve the dynamic quality of the reaching process, this work combines the exponential reaching law with the integral of Section 4.1, and proposes an integral reaching law, as shown in (32).

$$\frac{ds}{dt} = -[(1 - e^{-\beta|s|})(\varepsilon + k|s|) + k_i e^{-\beta|s|}|\int_0^t x_1 d\tau|]sgn(s) \tag{32}$$

where, $0 < \alpha < 1$, $\beta > 0$, $k_i > 0$.

The brackets in (32) contains two parts: the original exponential reaching law and the integral of x_1. The original exponential reaching law multiplies with $1 - e^{-\beta|s|}$, and the integral of x_1 multiplies with $e^{-\beta|s|}$. When the system state variable x_1 is far away from the sliding surface, $|s|$ is relatively large, $e^{-\beta|s|} \approx 0$, and $(1 - e^{-\beta|s|}) \approx 1$. At this time, the reaching law of (32) is similar to the exponential reaching law, which can enhance the reaching speed. As the system approaches the sliding surface, $|s\ |$ becomes smaller and smaller. When $|s|$ is very small, $e^{-\beta|s|} \approx 1$, $(1 - e^{-\beta|s|}) \approx 0$, and the integral of x_1, which plays a major role, is used to weaken the steady-state error.

It is expected that $e^{-\beta|s|}$ and $1 - e^{-\beta|s|}$ are always between 0 and 1, so the absolute value sign is added to s in the exponential part. In addition, to guarantee that the generalized sliding mode condition ($s \cdot ds/dt < 0$) is not affected by the integral of x_1 (the integral of x_1 maybe positive or negative), the integral of x_1 is added with an absolute value sign, and the sum of the two parts multiplies with the sign function $sgn\ (s)$.

To reduce the chattering and further increase the reaching speed, similar to the power reaching law, the above reaching law multiplies with $|s|^\alpha$, then (33) is obtained.

$$\begin{aligned}\frac{ds}{dt} = -[(1 - e^{-\beta|s|})(\varepsilon + k|s|) + k_i e^{-\beta|s|}|\int_0^t x_1 d\tau|]\\ \cdot |s|^\alpha sgn(s)\end{aligned} \tag{33}$$

Similar to Section 3.1, the control output of SMC-P can be calculated in (34). The proposed SMC-P doesn't rely on the complete information about the state of the HCSs and the disturbances. Only the information of T_G *and* $COMRATE_m$ is needed to calculate the control output of SMC-P, which impose a great flexibility to real applications.

$$\begin{aligned}u = fr + T_G\frac{dfr}{dt} + T_G[(1 - e^{-\beta|s|})(\varepsilon + k|s|)\\ + k_i e^{-\beta|s|}|\int_0^t x_1 d\tau|]|s|^\alpha sgn(s)\end{aligned} \tag{34}$$

V. SIMULATION ANALYSIS

To verify the performance of SMC-P, an uncertain nonlinear HCS in container ports with fluctuant f_1 and f_2 is simulated. In this work, we use the integral of time multiplied by the absolute error (*ITAE*) as a benchmark to understand the resilience for an uncertain nonlinear HCS in container ports. f_1 and f_2 are sinusoidal signals with offset, shown in the flowing (35-36):

$$f_1 = f_{10} + A_1 \cdot \sin(\omega_1 t + \varphi_1) \tag{35}$$

$$f_2 = f_{20} + A_2 \cdot \sin(\omega_2 t + \varphi_2) \tag{36}$$

where, $f_{10} = 0.05$, $A_1 = 0.005$, $\omega_1 = 1$, $\varphi_1 = \pi/6$, $f_{20} = -0.1$, $A_2 = 0.001$, $\omega_2 = 1.5$, and $\varphi_2 = -5\pi/12$.

Four methods, traditional method (TM), genetic algorithm (GA)(Luigi *et al.*, 2020)[33], quasi-sliding mode control (QSMC) and ISMC, are employed to compare with SMC-P. In this nonlinear HCS in container ports, $T_G = 2$, $T_Q = 1.5$, $T_F = 3$, $T_U = 0.5$, $T_I = 0.5$, and $COMRATE_m = 1.3$. TM is directly simulated in the nonlinear HCS in container ports, as shown in FIGURE 2. In GA method, T_G and T_Q are fixed value, while T_F,

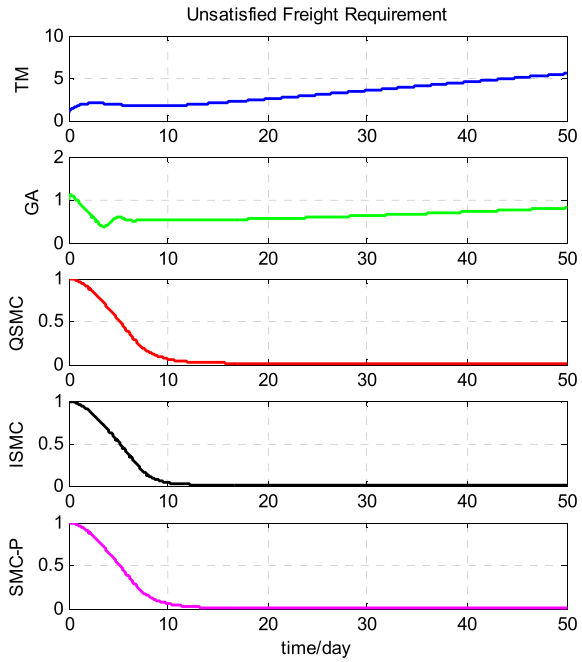

FIGURE 3. Comparison of *ufr* among five methods.

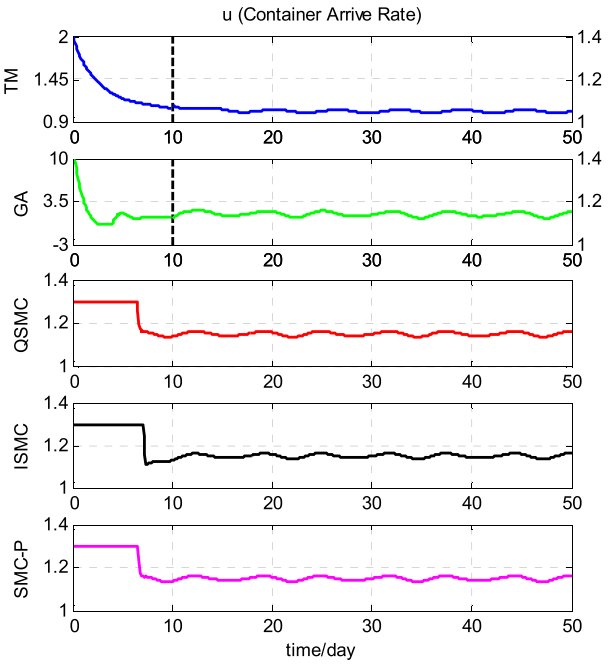

FIGURE 4. Comparison of control signal among five methods.

T_U, and T_I are optimized with *ITAE* of *ufr* as the fitness function. The ranges of T_F, T_U and T_I are [3,30], [0.1,7] and (0,1], respectively. In QSMC and ISMC, the exponential reaching law in (10) is employed and the saturation function is used to replace sign function to reduce chattering. According to (10), $\varepsilon = 0.5$, $\Delta = 0.05$, $k = 1$ in QSMC and ISMC; and according to (33), $\alpha = 0.8$, $\beta = 4$ in SMC-P.

The initial values of *ufr*, *arate*, and *comrate* are 1, 0 and 0, respectively. It is expected that unsatisfied freight requirement would reduce to 0, or as small as possible. All experiments were performed by MATLAB 7.1 on a computer equipped with an Intel Core i7, 3.6 GHz CPU and 12 GB RAM.

A. FR IS A STEP SIGNAL

In this section, fr is a step signal:

$$fr = fr_0 \cdot 1(t) \tag{37}$$

where, $fr_0 = 1$. The best T_F, T_U and T_I obtained by GA method are: $T_F = 12.3169$, $T_U = 0.1$ and $T_I = 1$. According to the switching function $s = c_1x_1 + x_2 + c_2\int x_1 dt$, $c_2 = 2$ in ISMC; and according to (33), $k_i = 1.6$ in SMC-P.

The comparisons of *ufr* and control signal u (in this uncertain nonlinear HCS, control signal is *arate*) among five methods are plotted in FIGUREs 3 and 4 respectively. In the 1st and 2nd subfigures of FIGURE 4, the ordinate of the curve for the first 10 days is on the left, while the ordinate of the curve for the last 40 days is on the right. The thick dashed line is the dividing line. The ordinate on the left can completely present the initial curve, and the ordinate on the right is consistent with other subfigures to promote convenient comparison among these subfigures. Steady-state error, settling time (t_s) and *ITAE* of five methods are given

TABLE 2. Steady-state error, Settling time and *ITAE*.

Method	TM	GA	QSMC	ISMC	SMC-P
e_m	5.5211	0.8215	0.0141	0.0083	0.0024
t_s	—	—	14.3	10.4	12.3
ITAE	4862.201	848.075	34.400	25.448	20.632

in TABLE 2. In TABLE 2, e_m, which is the maximum value of *ufr* in the 30th to 50th days, is used to describe the steady-state error. t_s is measured by taking 0.02 as the benchmark of *ufr*'s error, which is the same as that in the following subsection B. Because *ufr* obtained by TM and GA are always larger than 0.02, there is no data of t_s in the columns of TM and GA. *ITAE* is only calculated for the first 50 days.

From FIGURE 3, *ufr* obtained by TM does not increase significantly before the 10th day, while *ufr* obtained by GA decrease in the first few days. However, both of them continue to increase after the 10th day and cannot converge to a certain value. It is because *comrate* is easily smaller than the sum of *fr* and f_1, due to $f_2 < 0$. *ufr* obtained by other three methods can converge to certain values close to 0. The convergence speeds of *ufr* obtained by ISMC and SMC-P are faster than that obtained by QSMC.

From FIGURE 4, control signal u obtained by TM starts to decrease gradually from 2 and then fluctuates in a range slightly larger than 1. u obtained by GA first falls fast from 10 and then continues to fluctuate. Within the last 40 days, u obtained by GA is not much different from those obtained by the latter three methods. The waveforms of u obtained by the other three methods remain at 1.3 at the beginning and then fluctuate because of interference signals f_1 and f_2. There is a significant chattering between these two stages in u obtained by ISMC. The switching process between these two stages in u obtained by QSMC and SMC-P are much smoother.

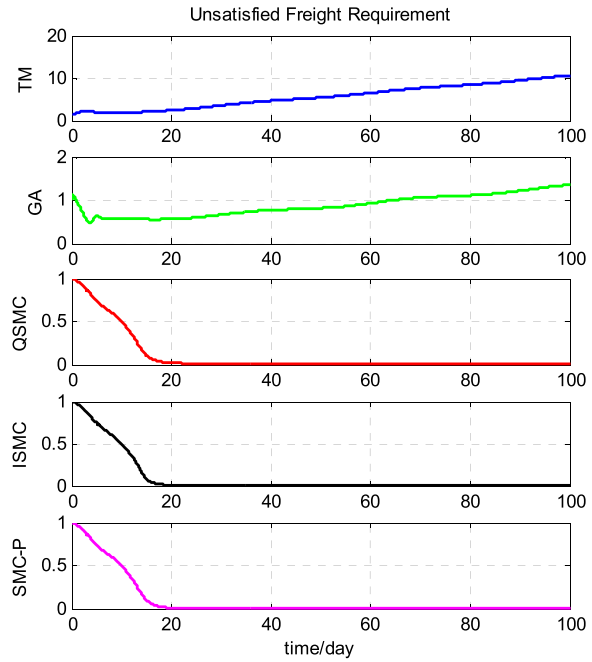

FIGURE 5. Comparison of *ufr* among five methods.

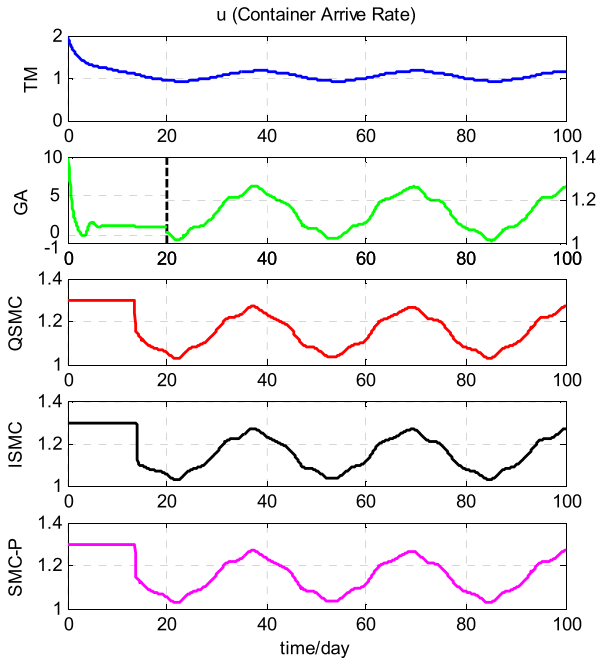

FIGURE 6. Comparison of control signal among five methods.

From TABLE 2, e_{m} obtained by TM and GA are much larger than those obtained by the other three methods. It can be calculated that e_{m} obtained by QSMC, 0.0141, is equal to $f_{h2} \cdot \Delta / c_1(\varepsilon + \Delta \cdot k)$ in (24), which is the maximum value of $\lim_{t\to\infty} ufr(t)$. e_{m} obtained by SMC-P is obviously smaller than those obtained by QSMC and ISMC. t_s obtained by QSMC is longer than those obtained by ISMC and SMC-P. t_s obtained by SMC-P is a bit longer than that obtained by ISMC. The relationship between *ITAE* of these five methods is similar to that of e_{m}. *ITAE* obtained by SMC-P is the smallest in those obtained by five methods.

B. FR IS A SINUSOIDAL SIGNAL WITH OFFSET

In this section, *fr* is a sinusoidal signal with offset:

$$fr = fr_0 + A \cdot \sin(\omega t + \varphi) \tag{38}$$

where, $A = 0.1$, $\omega = 0.2$, $\varphi = 0$. The best T_F, T_U and T_I obtained by GA method are 13.3959, 0.1 and 1, respectively. c_2 and k_i are the same as those in the subsection A of this part. *ufr* and control signal u obtained by five methods are plotted in FIGUREs 5 and 6 respectively. Similar with FIGURE 4, in the 2nd subfigure of FIGURE 6, the ordinate of the curve for the first 20 days is on the left, while the ordinate of the curve for the last 80 days is on the right. e_{m}, t_s and *ITAE* of five methods are given in TABLE 3. In TABLE 3, e_{m} is the maximum value of *ufr* in the 60th to 100th days. Same as subsection A, there is no data of t_s in the columns of TM and GA. *ITAE* is only calculated for the first 100 days.

From FIGURE 5, *ufr* obtained by TM and GA, which continue to increase, cannot converge to a certain value. It is because *comrate* is easily smaller than the sum of *fr* and f_1, due to $f_2 < 0$. *ufr* obtained by other three methods can converge to certain values close to 0. The convergence speeds of *ufr* obtained by ISMC and SMC-P are faster than that obtained by QSMC. There is little difference between waveforms of *ufr* obtained by ISMC and SMC-P.

TABLE 3. Steady-state error, Settling time and *ITAE*.

Method	TM	GA	QSMC	ISMC	SMC-P
e_{m}	10.6573	1.3625	0.0141	0.0105	0.0027
t_s	—	—	20.7	18	18.7
ITAE	35991.201	5037.832	122.317	102.807	68.609

From FIGURE 6, control signal u obtained by TM starts to decrease gradually from 2 and then fluctuates in a range slightly larger than 1. u obtained by GA first falls fast from 10 and then continues to fluctuate. Within the last 80 days, u obtained by GA is not much different from those obtained by the latter three methods. The waveforms of u obtained by the other three methods are similar with each other in all 100 days. They remain at 1.3 at the beginning and then fluctuate. In the switching process of these two stages, the waveforms of u obtained by QSMC and SMC-P are smoother than ISMC.

From TABLE 3, e_{m} obtained by TM is much larger than those obtained by the other four methods. e_{m} obtained by QSMC is still equal to $f_{h2} \cdot \Delta / c_1(\varepsilon + \Delta \cdot k)$ in (24). e_{m} obtained by SMC-P is obviously smaller than that obtained by QSMC and ISMC. Although t_s obtained by ISMC is the shortest in these methods, t_s obtained by SMC-P is slightly longer than that obtained by ISMC. *ITAE* obtained by SMC-P is obviously smaller than those obtained by other four methods.

Overall, both ISMC and SMC-P can reduce steady-state error in nonlinear handling chain systems with interferences. ISMC and SMC-P are obviously better than TM, GA and QSMC in steady-state error, settling time and resilience. In general, SMC-P is better than ISMC. However, these are

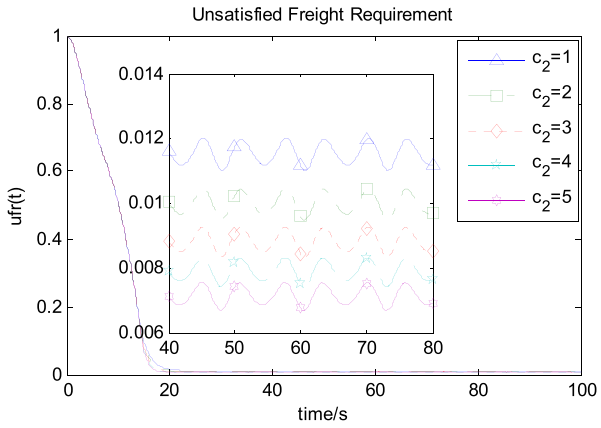

FIGURE 7. *ufr* obtained by ISMC with different c_2.

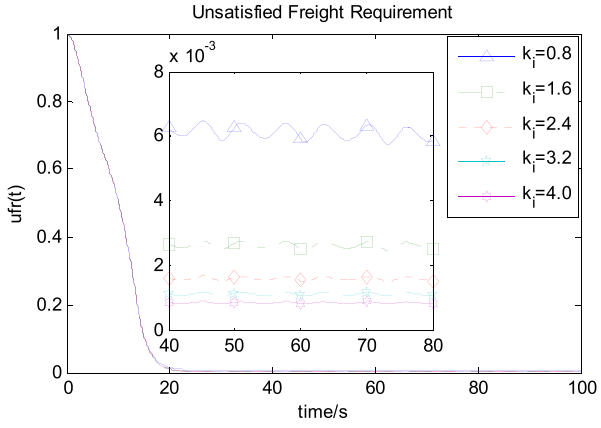

FIGURE 8. *ufr* obtained by SMC-P with different k_i.

only comparisons between ISMC and SMC-P under certain parameters. To confirm whether SMC-P is better or not, detailed comparisons between ISMC and SMC-P under various parameters are shown in the following Section.

C. DETAILED COMPARISONS BETWEEN ISMC AND SMC-P

In this subsection, detailed comparisons are made between the ISMC and SMC-P of taking several values for the parameters c_2 and k_i to validate the effectiveness of SMC-P. Except for parameters c_2 and k_i, other parameters are the same as the subsection B of this part.

In FIGUREs 7 and 8, *ufr* obtained by ISMC with different c_2 ($c_2 = 1$, 2, 3, 4 and 5) and SMC-P with different k_i($k_i =$ 0.8, 1.6, 2.4, 3.2 and 4.0) are plotted. To distinguish the steady-state error and fluctuation with different parameters, the values of *ufr* from the 40^{th} day to the 80^{th} day are drawn in the subgraphs. In FIGUREs 9 and 10, the values of control signal u obtained by ISMC with different c_2 and SMC-P with different k_i are given. In FIGURE 11, the values of steady-state error obtained by ISMC with different c_2 and SMC-P with different k_i are compared. In FIGURE 10, the values of *ITAE* obtained by ISMC with different c_2 and SMC-P with different k_i are compared. In FIGUREs 11 and 12, the abscissas above and below belong to c_2 of ISMC and k_i of SMC-P respectively. The left and right ordinates are the same.

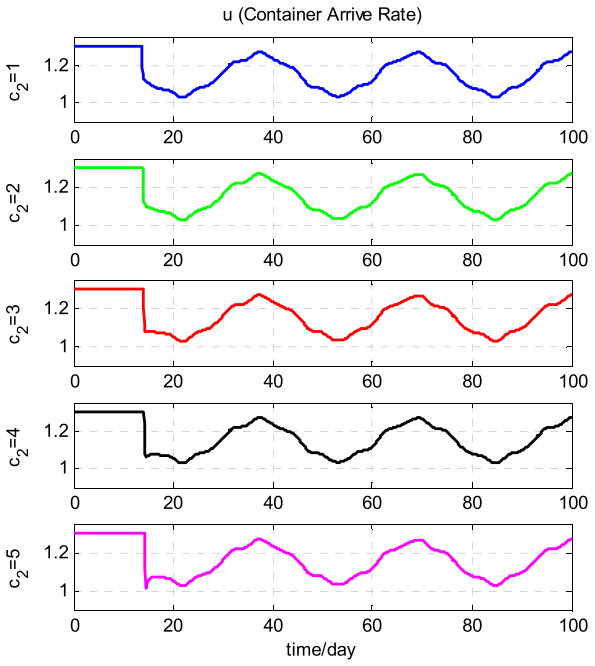

FIGURE 9. Control signal obtained by ISMC with different c_2.

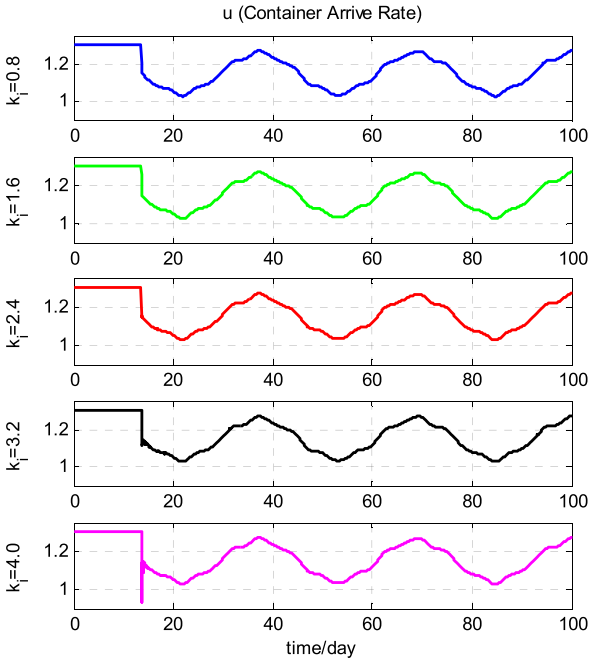

FIGURE 10. Control signal obtained by SMC-P with different k_i.

From FIGUREs 7 and 8, the overall change trends of *ufr* obtained by two methods with different parameters are not much different. However, it can be seen from the sub-graphs that the steady-state errors are different under various parameters. In *ufr* obtained by ISMC, the larger c_2, the smaller the steady-state error. In *ufr* obtained by SMC-P, the larger k_i, the smaller the steady-state error. The steady-state errors of *ufr* obtained by SMC-P are smaller than those of *ufr* obtained by ISMC. The fluctuation of *ufr* obtained by SMC-P is obviously less than that of obtained by ISMC.

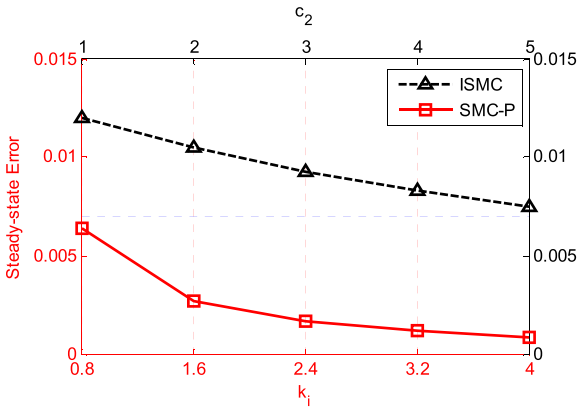

FIGURE 11. Steady-state error obtained by ISMC and SMC-P.

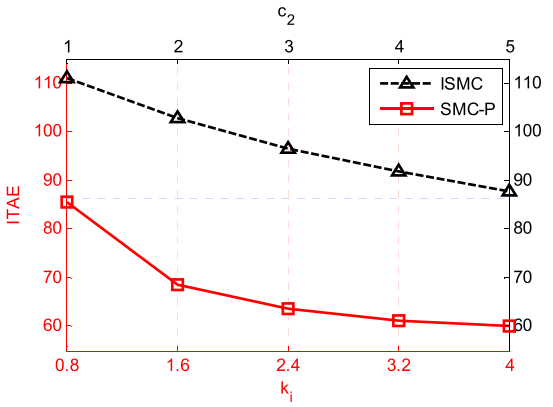

FIGURE 12. *ITAE* obtained by ISMC and SMC-P.

From FIGUREs 9 and 10, the curves of u are relatively smooth with no chattering when c_2 and k_i are smaller, such as $c_2 = 1$ and 2, $k_i = 0.8$, 1.6 and 2.4. However, the chattering between the 10^{th} day and the 20^{th} day become more and more serious with the increase of the parameters c_2 and k_i, such as $c_2 = 3$, 4 and 5, $k_i = 3.2$ and 4.0.

From FIGUREs 11 and 12, the steady-state error and *ITAE* obtained by ISMC or SMC-P gradually decrease as c_2 or k_i increases. The values of steady-state error and *ITAE* obtained by ISMC are greater than those obtained by SMC-P. The minimum steady-state error and *ITAE* obtained by ISMC are still larger than the maximum steady-state error and *ITAE* obtained by SMC-P.

In general, although both ISMC and SMC-P can reduce steady-state errors, SMC-P achieves better results than ISMC in considering the trade-off between steady-state error reduction and chatter avoidance. Therefore, it is validated that SMC-P outperforms ISMC in the aspects of performance, robustness and resilience when dealing with the nonlinear HCS of container ports under uncertainty. However, there is the same phenomenon between SMC-P and ISMC that deserves the attention of container port operators. That is, with the gradual increase of parameters, the steady-state error gradually decreases, while the chattering may appear and become more serious. In the operation of container ports, how to select the appropriate parameters requires reasonable consideration for the two factors in accordance with the planning and management objectives.

Through comparing (12) with (34), the computational complexity of the proposed SMC-P increases more slightly than that of ISMC and QSMC. However, uncertain nonlinear model of handling chain system in container ports takes days as the unit, which highlights the calculation performance, while the increase of calculation time (seconds) may be ignored. Moreover, it is found through simulation that the SMC-P operation time is only 1.27 seconds. In view of the calculation time requirement of uncertain nonlinear HCS in container ports is not much high, the slight increase of time of the proposed SMC-P is acceptable. With respect to the calculation performance, the SMC-P outperforms other four methods in *ufr, u,* steady-state error, settling time and resilience. In addition, SMC-P does not only balance both steady-state error reduction and chattering avoidance, but also optimize the performance, robustness, and resilience of the uncertain nonlinear HCS.

VI. CONCLUSION

This work proposes a sliding mode control method with power integral reaching law for the uncertain nonlinear HCS in container ports. This method adds the integral of the system state variable to the reaching law to reduce steady-state errors, and uses the power reaching law to accelerate the reaching speed and weaken the chattering. Considering uncertain freight requirement and handling ability, simulations among five methods verify the effectiveness of SMC-P in the aspects of steady-state error, settling time and resilience; detailed comparisons between ISMC and SMC-P under various parameters show SMC-P can better achieve the trade-off between reducing the steady-state errors and weakening the chattering. The method proposed in this work meets the actual management and maintenance requirements of HCS in container ports. It helps port authorities to design more effective and competitive control decisions.

There are several directions s to further and improve the work, which can be considered as future avenues for research:

- Development in new advanced control approach

Despite the good performance of our proposed SMC-P in this work, there are novel ways to develop it further in order to obtain results better to achieve the trade-off between reducing steady-state errors and weakening chattering and in a shorter time. This can be done by combining other techniques, such as feedback linearization control, adaptive control, fuzzy control, or neural network into steps within the SMC.

- Extension into some complicated uncertainties

Uncertainties always exist in the real world; however, some complicated uncertainties cannot be represented just with parameters, e.g., disruption events, vessels backlogging, inaccuracy of container information, and equipment failure. Therefore, HCS in container ports considering complicated emergencies will be a valuable future research direction.

REFERENCES

[1] J. He, C. Tan, and Y. Zhang, "Yard crane scheduling problem in a container terminal considering risk caused by uncertainty," *Adv. Eng. Informat.*, vol. 39, pp. 14–24, Jan. 2019.
[2] B. Xu, J. Li, Y. Yang, H. Wu, and O. Postolache, "Model and resilience analysis for handling chain systems in container ports," *Complexity*, vol. 2019, pp. 1–12, Jul. 2019.
[3] F. Zheng, X. Man, F. Chu, M. Liu, and C. Chu, "A two-stage stochastic programming for single yard crane scheduling with uncertain release times of retrieval tasks," *Int. J. Prod. Res.*, vol. 54, no. 13, pp. 4132–4147. 2019.
[4] Q. Feng, X. Zhao, D. Fan, B. Cai, Y. Liu, and Y. Ren, "Resilience design method based on meta-structure: A case study of offshore wind farm," *Rel. Eng. Syst. Saf.*, vol. 186, pp. 232–244, Jun. 2019.
[5] B. Cai, M. Xie, Y. Liu, Y. Liu, and Q. Feng, "Availability-based engineering resilience metric and its corresponding evaluation methodology," *Rel. Eng. Syst. Saf.*, vol. 172, pp. 216–224, Apr. 2018.
[6] X.-L. Han, Z.-Q. Lu, and L.-F. Xi, "A proactive approach for simultaneous berth and quay crane scheduling problem with stochastic arrival and handling time," *Eur. J. Oper. Res.*, vol. 207, no. 3, pp. 1327–1340, Dec. 2010.
[7] J. Luo, Y. Wu, A. Halldorsson, and X. Song, "Storage and stacking logistics problems in container terminals," *OR Insight*, vol. 24, no. 4, pp. 256–275, Dec. 2011.
[8] G. A. E.-N.-A. Said and E.-S.-M. El-Horbaty, "An optimization methodology for container handling using genetic algorithm," *Procedia Comput. Sci.*, vol. 65, pp. 662–671, 2015.
[9] Y. Türkoğullari, Z. Taşkin, N. Aras, and I. Altinel, "Optimal berth allocation, time-variant quay crane assignment and scheduling with crane setups in container terminals," *Eur. J. Oper. Res.*, vol. 254, no. 3, pp. 985–1001, 2016.
[10] A. Ballis, J. Golias, and C. Abarkoumkin, "A comparison between conventional and advanced handling systems for low volume container maritime terminals," *Maritime Policy Manage.*, vol. 24, no. 1, pp. 73–92, 1997.
[11] A. Paixão and M. P. Bernard, "Fourth generation ports–a question of agility?" *Int. J. Phys. Distrib. Logistics Manage.*, vol. 33, no. 4, pp. 355–376. 2003.
[12] F. Facchini, G. Mummolo, G. Mossa, S. Digiesi, F. Boenzi, and R. Verriello, "Minimizing the carbon footprint of material handling equipment: Comparison of electric and LPG forklifts," *J. Ind. Manage. Optim.*, vol. 9, no. 5, pp. 1035–1046. 2016.
[13] C. Liang, L. Fan, D. Xu, Y. Ding, and M. Gen, "Research on coupling scheduling of quay crane dispatch and configuration in the container terminal," *Comput. Ind. Eng.*, vol. 125, pp. 649–657, Nov. 2018.
[14] Ç. Iris and J. S. L. Lam, "Recoverable robustness in weekly berth and quay crane planning," *Transp. Res. Part B: Methodol.*, vol. 122, pp. 365–389, Apr. 2019.
[15] H. Aytug, M. A. Lawley, K. McKay, S. Mohan, and R. Uzsoy, "Executing production schedules in the face of uncertainties: A review and some future directions," *Eur. J. Oper. Res.*, vol. 161, no. 1, pp. 86–110, Feb. 2005.
[16] F. Facchini, S. Digiesi, and G. Mossa, "Optimal dry port configuration for container terminals: A non-linear model for sustainable decision making," *Int. J. Prod. Econ.*, vol. 219, pp. 164–178, Jan. 2020.
[17] L. Zhen, "Yard template planning in transshipment hubs under uncertain berthing time and position," *J. Oper. Res. Soc.*, vol. 64, no. 9, pp. 1418–1428, Sep. 2013.
[18] M. Golias, I. Portal, D. Konur, E. Kaisar, and G. Kolomvos, "Robust berth scheduling at marine container terminals via hierarchical optimization," *Comput. Oper. Res.*, vol. 41, pp. 412–422, Jan. 2014.
[19] A. Mhalla, S. C. Dutilleul, and H. Zhang, "Robust control under uncertainty for seaport handling equipments," *Transp. Res. Procedia*, vol. 14, pp. 203–212, 2016.
[20] B. Xu, J. Li, Y. Yang, H. Wu, and O. Postolache, "A novel sliding mode control with low-pass filter for nonlinear handling chain system in container ports," *Complexity*, vol. 2020, pp. 1–15, Feb. 2020.
[21] Y. Han, Y. Kao, and C. Gao, "Robust sliding mode control for uncertain discrete singular systems with time-varying delays and external disturbances," *Automatica*, vol. 75, pp. 210–216, Jan. 2017.
[22] G. P. Incremona, G. De Felici, A. Ferrara, and E. Bassi, "A supervisory sliding mode control approach for cooperative robotic system of systems," *IEEE Syst. J.*, vol. 9, no. 1, pp. 263–272, Mar. 2015.
[23] A. Khanzadeh and M. Pourgholi, "Fixed-time sliding mode controller design for synchronization of complex dynamical networks," *Nonlinear Dyn.*, vol. 88, no. 4, pp. 2637–2649, Jun. 2017.
[24] S. Mobayen and J. Ma, "Robust finite-time composite nonlinear feedback control for synchronization of uncertain chaotic systems with nonlinearity and time-delay," *Chaos, Solitons Fractals*, vol. 114, pp. 46–54, Sep. 2018.
[25] Y. Wang, X. Xie, M. Chadli, S. Xie, and Y. Peng, "Sliding mode control of fuzzy singularly perturbed descriptor systems," *IEEE Trans. Fuzzy Syst.*, early access, May 29, 2020, doi: 10.1109/TFUZZ.2020.2998519.
[26] S. Mobayen, "Design of LMI-based sliding mode controller with an exponential policy for a class of underactuated systems," *Complexity*, vol. 21, no. 5, pp. 117–124, 2016, doi: 10.1002/cplx.21636.
[27] Y. Wang, Y. Xia, H. Li, and P. Zhou, "A new integral sliding mode design method for nonlinear stochastic systems," *Automatica*, vol. 90, pp. 304–309, Apr. 2018.
[28] S. Mobayen, M. J. Yazdanpanah, and V. J. Majd, "A finite-time tracker for nonholonomic systems using recursive singularity-free FTSM," in *Proc. Amer. Control Conf.*, San Francisco, CA, USA, Jun. 2011, pp. 1720–1725.
[29] P. Zhang, J. Hu, H. Liu, and C. Zhang, "Sliding mode control for networked systems with randomly varying nonlinearities and stochastic communication delays under uncertain occurrence probabilities," *Neurocomputing*, vol. 320, pp. 1–11, Dec. 2018.
[30] S. Mobayen and F. Tchier, "Nonsingular fast terminal sliding-mode stabilizer for a class of uncertain nonlinear systems based on disturbance observer," *Scientia Iranica*, vol. 24, no. 3, pp. 1410–1418, Jun. 2017.
[31] X. Liu, Z. Shan, and Y. Li, "Dynamic boundary layer based neural network quasi-sliding mode control for soft touching down on asteroid," *Adv. Space Res.*, vol. 59, no. 8, pp. 2173–2185, Apr. 2017.
[32] S. Saraeian, B. Shirazi, and H. Motameni, "Adaptive control of criticality infrastructure in automatic closed-loop supply chain considering uncertainty," *Int. J. Crit. Infrastruct. Protection*, vol. 25, pp. 102–124, Jun. 2019.
[33] L. Rarità, I. Stamova, and S. Tomasiello, "Numerical schemes and genetic algorithms for the optimal control of a continuous model of supply chains," *Appl. Math. Comput.*, vol. 388, Jan. 2021, Art. no. 125464, doi: 10.1016/j.amc.2020.125464.

BOWEI XU received the M.Sc. degree in transportation planning and management and the Ph.D. degree in logistics management and engineering from Shanghai Maritime University, Shanghai, China. Her current research interest includes logistics optimization in automation container terminal.

JUNJUN LI received the B.Sc., M.Sc., and Ph.D. degrees from Shanghai Maritime University, Shanghai, China. He is currently a Lecturer with the College of Merchant Marine, Shanghai Maritime University. His current research interest includes intelligent optimization.

YONGSHENG YANG received the Ph.D. degree from the Nanjing University of Aeronautics and Astronautics, in 1998. He is currently a Professor with the Institute of Logistics Science and Engineering, Shanghai Maritime University. His current research interests include port logistics operation and optimization, collaborative operation scheduling and control in automated terminals, and port logistics equipment and its intelligence.

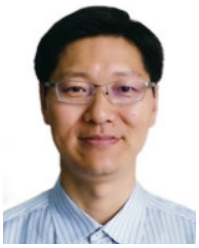

HUAFENG WU received the Ph.D. degree from Fudan University, in 2008. He is currently a Professor with the College of Merchant Marine, Shanghai Maritime University. His current research interests include computer, communication and networks, and traffic information engineering and control.

WEIHUI DAI (Member, IEEE) received the Ph.D. degree from Zhejiang University, China. He is currently a Professor with the School of Management, Fudan University. His research interests include information technology and information management.

OCTAVIAN POSTOLACHE (Senior Member, IEEE) received the Ph.D. degree from Gheorghe Asachi Technical University, Iaşi, Romania. He is currently a Professor with the Instituto de Telecomunicacoes, ISCTE-IUL. His research interest includes computational intelligence with application in automated measurement systems.